Continental Shelf Research 108 (2015) 112–120

Contents lists available at ScienceDirect

Continental Shelf Research

journal homepage: www.elsevier.com/locate/csr

Sediment resuspension in a shallow lake with muddy substrates: St Lucia, South Africa

Vulindlela Zikhali [a], Katrin Tirok [a,b], Derek Stretch [a,*]

[a] Centre for Research in Environmental, Coastal & Hydrological Engineering, School of Engineering, University of KwaZulu-Natal, Durban 4041, South Africa
[b] School of Life Sciences, University of KwaZulu-Natal, Durban 4041, South Africa

ARTICLE INFO

Article history:
Received 31 March 2015
Received in revised form
17 July 2015
Accepted 12 August 2015
Available online 18 August 2015

Keywords:
SSC
Bed composition
Wind waves
Estuary
Coastal lagoon
Turbidity
Mathematical model

ABSTRACT

Wind-driven sediment resuspension affects the physical and biological environment of the water column in shallow estuarine lakes. This study investigated the relationship between wind-driven waves and suspended sediment concentration (SSC) using the 33 km^2 South Lake basin of Lake St Lucia, South Africa as a case study. Five wave poles measuring significant wave height and turbidity were deployed over an aggregate period of twenty days at distributed locations where sediment substrate compositions varied from muddy to sandy and depths ranged from 0.7 m to 2.1 m. The resulting turbidity dynamics were used to test a simple depth-averaged model of suspended sediment concentrations. The model performed best in the muddy regions of the lake and was able to simulate the resuspension dynamics more accurately than the settling dynamics. Peak suspended sediment concentration levels were best captured for the deeper muddy locations. The model provides a means to make spatially explicit predictions of suspended sediment concentrations that can be used to understand the forcing mechanisms for primary producer growth and distribution or to improve sediment budget calculations.

1. Introduction

The suspended sediment concentration (SSC hereinafter) has a marked effect on the water column's physical and chemical properties, ecology and benthic geomorphology (Cloern, 1987; Liu et al., 2014; Wu and Hua, 2014). The water quality of a shallow lake is directly affected by sediment resuspension and SSC. Resuspension enhances phosphorous release from the sediment which can also increase potential eutrophication (Scheffer, 1998). Light attenuation caused by high SSC and high turbidity affects phytoplankton and macrophyte productivity and species' distribution (Cloern, 1987; Bailey and Hamilton, 1997) while zooplankton may experience reduced feeding and increased mortality rates (Carrasco et al., 2013).

The dynamics of cohesive sediments has been widely investigated since the 1960s due to its importance in the health and biophysical functioning of hydro-ecosystems. Overviews are given by Dyer (1986), Healy et al. (2002), Wolanski (2007), and Partheniades (2009). It is well known from these studies that sediment resuspension is linked to wave and current induced shear stresses near the bed. Bed shear stresses are in turn related to water depths, current speeds, wave amplitudes and wave periods (e.g. Bailey and Hamilton, 1997; Brand et al., 2010, amongst many others). When bed shear stresses exceed a critical value sediment is displaced from the bed and distributed into the water column by turbulence (e.g. Ravens, 1997; Green, 2011). The critical value depends on the bed erodibility, which is influenced by a multitude of factors including both physical and biological characteristics (e.g. Lundkvist et al., 2007). Bed erodibility is generally higher for soft muddy substrates compared to more consolidated sandy substrates. Biofilms composed of microalgae and bacteria may stabilise the sediment surface. In contrast, zoobenthos may increase erodibility through bioturbation (e.g. burrowing organisms) or increased bed roughness arising from sessile organisms (e.g. mussels) or from structures such as tracks and mounds of motile organisms. Such biological factors may be particularly important in productive estuarine and shallow lake systems (Le Hir et al., 2007). These systems often have muddy benthic substrates due to sedimentary infilling of silt and clays from the surrounding area, fluvial sources and slow-moving currents (Castaing and Allen, 1981). This enhances resuspension by wind driven waves and causes high turbidities.

The modelling of suspended sediment dynamics enables us to anticipate and understand the reaction of the biological and physical environment within shallow lakes. Brand et al. (2010) and Qian et al. (2011) note how sediment resuspension may be linked directly to wind speed, except where advective currents have a significant influence since waves and currents may sometimes

* Corresponding author. Fax: +27 31 2601411.
E-mail address: stretchd@ukzn.ac.za (D. Stretch).

http://dx.doi.org/10.1016/j.csr.2015.08.012
0278-4343/

develop independently. Previous research has modelled suspended sediment dynamics driven by wind-waves in large (> 600 km^2) shallow lakes such as Lake Balaton in Hungary (Luettich et al., 1990), Lake Okeechobee in the USA (Jin and Ji, 2001), Lake Taihu in China (Wu et al., 2013), as well as for smaller systems (< 60 km^2) such as Esteros del Ibera in Argentina (Cozar et al., 2005). These models can help us understand sediment redistribution and associated water quality issues such as the effects on primary production. They can also assist in assessing the benefits of sediment input management.

The Luettich et al. (1990) model is an example of a simple sediment resuspension model that may be applicable to shallow lakes with muddy substrates. It is a depth-averaged box model that can incorporate the effects of wind-generated waves, bed sediment characteristics, and suspended sediment settling velocities to predict suspended sediment concentrations under local equilibrium conditions where advection effects are relatively small.

For our study we used the model by Luettich et al. (1990) to describe sediment dynamics driven by wind induced waves in a shallow estuarine lake system, Lake St Lucia, in South Africa. Lake St Lucia is part of the iSimangaliso Wetland Park, a world heritage site and one of the largest estuarine systems in Africa (Lawrie and Stretch, 2011a; Perissinotto et al., 2013). The estuarine system is of high ecological and touristic importance serving as a nursery ground for many fish species and prawns that are sustained by a productive planktonic and benthic food web (Benfield et al., 1990; Whitfield et al., 2006). Strong winds and the lake's large surface area (~ 330 km^2) and shallow depth (~1 m) lead to generally high turbidities (>50 NTU or nephelometric turbidity units) with peak values up to 1000 NTU (Cyrus, 1988; Mackay et al., 2010). Understanding the dynamics of suspended sediment concentration in such shallow systems gives insight into their ecological functioning and can support management decisions in the context of climate change.

For the present study we measured wind-driven waves and the associated dynamics of suspended sediment concentrations (SSC) at the St Lucia case study site. The aim was to improve our understanding of the processes and to test whether a simple depth-averaged model can accurately predict the resuspension dynamics in a shallow lake with complex morphology and non-homogeneous bed sediments.

2. Methods

2.1. Case study site

Lake St Lucia is located in northern KwaZulu-Natal on the eastern coast of South Africa (28°00′25.96″S, 32°28′50.58″E) and comprises three interconnected basins – False Bay, North Lake and South Lake (Fig. 1). The lake is linked to the sea by a 22 km long sinuous channel called the Narrows. The inlet from the sea can close for prolonged time periods due to near-shore littoral transport processes (Lawrie and Stretch, 2011a,b; Perissinotto et al., 2013). Tidal effects are present for about 14 km up the Narrows when the inlet is open – the lake itself is not tidal.

The lake has a surface area of approximately 328 km^2 and an average depth of 1.0 m when the inlet is open and when water levels are near the estuary mean water level (EMWL), a local datum that is 0.25 m above sea level (Lawrie and Stretch, 2011a). When the inlet is closed the water level can differ strongly from EMWL depending on rainfall, river inflow and evaporation. Field work was carried out in the southern half of South Lake (Fig. 1) between April 2013 and January 2014. The inlet of Lake St Lucia was closed throughout our study period, thus net outflow of the system was zero. The average water level was ±0.3 m above EMWL during this period. The southern basin of South Lake has a surface area of approximately 30 km^2, extending approximately 6 km from north to south and 5 km east to west. The bed sediments vary spatially and generally comprise sandy regions around the edges with finer sediments in the deeper areas (Fig. 1(b)). Cyrus (1988) noted how the water in South Lake is known to be clear in the east and turbid to the west which suggests a spatial difference in resuspension dynamics.

The lake system may exhibit high benthic algal production and significant biofilms during dry periods with very low water levels (Perissinotto et al., 2013). Common macrozoobenthos species occurring in Lake St Lucia include bivalves such as *Solen cylindraceus* and *Brachidontes virgiliae* as well as crustaceans and polychaetes which may influence erodibility of the sediment (Mackay et al., 2010; Perissinotto et al., 2013). Studies investigating potential effects of biology on sediment characteristics in Lake St Lucia are however not available.

The wind climate at St Lucia is characterised by prevailing north-easterly and south-westerly winds that drive significant inter basin water exchanges between North and South Lake (Hutchison and Pitman, 1977; Schoen et al., 2014). There is a strong diurnal cycle in the wind. Wind speeds during the day are typically 4 m s^{-1} or higher, whereas during the night they tend to be below 4 m s^{-1}.

2.2. Field measurements

Waves and turbidity were measured at several locations (Fig. 1 (b)) for an aggregate period of 20 days between April 2013 and January 2014. Wave time series were obtained from wave poles located throughout South Lake (Zikhali et al., 2014). Wave-induced pressures were logged using pressure transducers at a burst sampling frequency of 4 Hz for durations of 5 min (1200 readings) every 15 min. The pressure transducers and their digital microcontrollers were sealed in plastic bags and mounted inside the top of the perforated wave poles (Fig. 1(c)). Turbidity (NTU) was also measured at 15 min intervals using YSI multi-parameter water quality sondes (models 6920 V2 and EXO2). The YSI sondes were attached to the wave poles at depths that ensured submergence in high wave conditions, but near enough to the surface to allow daily inspection from a boat. In addition to turbidity, the sondes also recorded salinity and dissolved oxygen but that data will not be presented. It is however worth noting that salinities increased steadily during the course of the field experiments due to the low fresh water inputs into the system. Salinity in April 2013 was in the range 6.3–6.8 increasing to 9.5–11 in July 2013 and 11–13 in January 2014.

In April 2013 wave pole AP3 was located in a region of predominantly sand/mud bottom sediments with an average depth of 1.5 m (see Fig. 1). Two wave poles were deployed in July 2013, one in the sandy region in the north of the South Lake basin at 0.9 m depth (JP0) and the second in the deeper, muddier central region at 2.1 m depth (JP3). In January 2014 wave pole JAN3 was positioned in the same sandy region as JP0. The turbidity measurements during this period were taken from a turbidometer positioned at JAN2 (Fig. 1), approximately 800 m from the wave measurement pole, because the turbidometer at JAN3 malfunctioned. The water depth at each wave pole was measured during deployment of the pole using a surveying staff to cross-check the average depth recorded by the wave pressure transducers. Water levels were periodically recorded near the weather station using a surveying staff attached to a jetty. Sediment core samples were collected at each wave pole site for particle size analysis using a Malvern Mastersizer 2000 (Table 2). Particles <63 μm in diameter were classified as mud and particles ≥63 (up to a maximum recordable size of 2000 μm) as sand following Folk (1954). Water

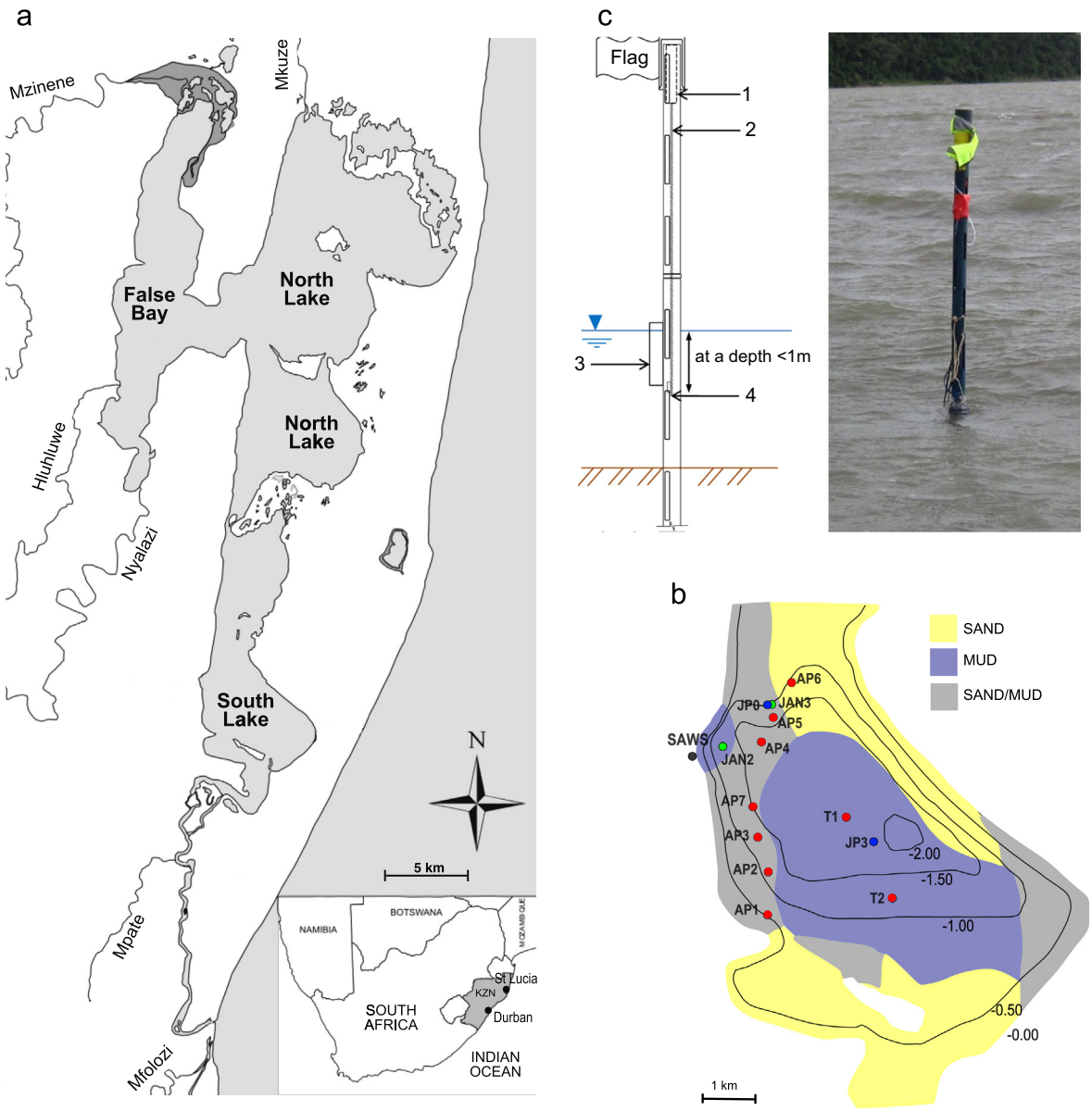

Fig. 1. (a) Map of St Lucia estuarine lake system on the east coast of South Africa. (b) Detailed map of the southern basin showing bathymetry, substrate distribution (after Fortuin, 1992; Perissinotto et al., 2013), location of wave poles and sampling stations (APx and Tx – stations used in April 2013, JPx – stations used in July 2013, and JANx – stations used in January 2014 (for details see Section 2.2), and location of the weather station (SAWS). (c) Schematic diagram of the wave pole components. The labelled items are: (1) differential pressure transducer device and data logger, (2) plastic manometer tube, (3) YSI multiparameter sonde and (4) end of manometer tube with weight.

samples were collected from the top and bottom layer of the water column at sites AP2, AP3, AP5, AP6, T1 and T2 in April 2013 and site JAN2 in January 2014 for particle size analysis using the Malvern.

A relationship between turbidity and SSC was established using a sediment sample (top 1 cm) from the muddy central region of South Lake. Increasing amounts of sediment were suspended in water to achieve different turbidity levels between 1 and 1000 NTU. Duplicate water samples were taken at each turbidity level and filtered through pre-weighed 0.2 μm glass fibre filters. The filters were then dried and re-weighed to obtain a SSC measurement and thus derive a calibration curve. D_{50} particle size of the calibration sediment ranged between 11 and 14 μm, similar to the range for in situ water samples from different sites throughout the lake (D_{50} = 7–13 μm, cf. Table 3). Turbidity readings of the two YSI probes agreed well with each other. The SSC – turbidity relationship derived was SSC (mg l^{-1}) = 1.4 NTU (R^2 = 0.99). The same relationship between SSC and turbidity was used for all sites. Vertical turbidity profiles were also measured intermittently at various locations throughout the lake (AP1–AP7, cf. Fig. 1(b)) to investigate whether a vertical turbidity gradient existed and whether the assumption of uniform mixing was valid.

2.3. Data analysis

Recorded pressure data was used to derive significant wave heights (H_s) for each 5 min sampling period. The pressure time series were decomposed into Fourier modes, each with a specific frequency. These modes were individually corrected for attenuation of the pressure with depth according to linear wave theory. An inverse Fourier transform was then used to reconstruct the time series of actual water surface displacements (for details see Zikhali et al., 2014). Significant wave heights H_s were then estimated from these time series and used in a deterministic model to establish the wave-induced model SSC for comparison with the observed SSC (Luettich et al., 1990). The average depth at each pole

site was calculated from the mean pressure measured over each 5 min period (assuming a hydrostatic mean pressure distribution) and adding the depth below the transducer tube which was measured using a survey staff during pole deployment.

2.4. Model for suspended sediment concentrations (SSC)

The model developed by Luettich et al. (1990) describes suspended sediment dynamics in wave-influenced shallow lakes that are well mixed and where lateral advection is negligible. The model was developed and tested in the 600 km^2 Lake Balaton (Hungary) with an average depth of 3.2 m, and a bed comprised mainly of silt and clays.

Following Luettich et al. (1990) a simplified model for depth-averaged SSC based on a local sediment mass balance can be expressed as

$$\frac{dc}{dt} = -\frac{w_s}{h}(c - c_e) \tag{1}$$

where c is the depth-averaged sediment concentration, w_s is a sediment settling velocity, h is the water depth and c_e represents an equilibrium concentration where resuspension and settling processes are balanced in a steady state situation.

The concentration c_e is assumed to be predominantly wave-driven and related to the wave characteristics by

$$c_e = c_0 + K\left(\frac{H_s - H_c}{h}\right)^n \quad \text{for } H_s > H_c \tag{2}$$

$$c_e = c_0 \quad \text{for } H_s < H_c \tag{3}$$

where c_0 is a non-settling background concentration, K is a resuspension parameter that will in general depend on the substrate characteristics (i.e. is location specific), H_s is the significant wave height, H_c is a critical wave height below which no resuspension occurs, and h is the water depth. The exponent n is linked to the relationship between the wave induced bottom shear stress τ and the wave induced orbital velocity u. The shear stress may be expected to scale as $\tau \sim \rho u^2$, and for nearly monochromatic waves with a single dominant wave period this suggests $n \approx 2$.

Values for K can be informed by those estimated by Luettich et al. (1990) since their bed material sediment size distributions were similar to those at our case study site. However we note that Luettich et al. (1990) used a slightly different form of Eq. (2) that included an arbitrary reference wave height H_{ref} in place of the water depth h. The K parameter used here can be related to that of Luettich by

$$K_{Luett} = K\left(\frac{H_{ref}}{h}\right)^n \tag{4}$$

Sediment settling velocity is known to vary with sediment concentration and particle size as well as salinity and organic matter content through the process of flocculation (Luettich et al., 1990; Mikes et al., 2002; Partheniades, 1965, 2009). In this study we followed Luettich's approach of a constant settling velocity over time and across sites. Salinity throughout our field experiment was >6 and thus likely always within the range where flocculation occurs in Lake St Lucia (Maine, 2011). Thus, the effect of flocculation is implicitly included in the settling velocity.

Assuming that c_e, w_s and h are constant during each time step Δt (taken as 15 min in this study), integrating Eq. (1) over the time interval $(t, t + \Delta t)$ yields a difference equation

$$c(t + \Delta t) = c(t)e^{-w_s \Delta t/h} + c_e(t)(1 - e^{-w_s \Delta t/h}) \tag{5}$$

which can be used to predict the SSC concentration given the local wave height H_s, water depth h and model parameters K, H_c, w_s.

The model parameters (Table 4) were estimated by iteratively minimising the mean squared differences between the modelled and observed data. The values for H_c, w_s, c_0 and n were assumed to be the same for all sites with only the parameter K allowed to vary to account for different bed characteristics and related factors. A settling velocity of 0.02 cm s^{-1} was inferred from this process and is consistent with results previously obtained by Maine (2011) who analysed suspended sediment samples collected from South Lake. A constant value of background concentration $c_0 = 15$ mg l^{-1} was inferred from measured turbidity data during calm periods. This background value is attributed to particles that settle much slower than the majority of the particles in the water column. Slow settling particles may include micro-flocs and planktonic organisms.

An error analysis was used to elucidate conditions under which the model performed best. It was based on the root mean square errors and an agreement index (Willmott, 1981) and efficiency index (Legates and McCabe, 1999). The agreement index is a normalised measure of agreement between the modelled and observed data and ranges between 0 (poor) and 1 (perfect). The coefficient of efficiency ranges from negative infinity to 1 with higher values indicating better model performance and negative values indicating that the observed mean is a better predictor than the model.

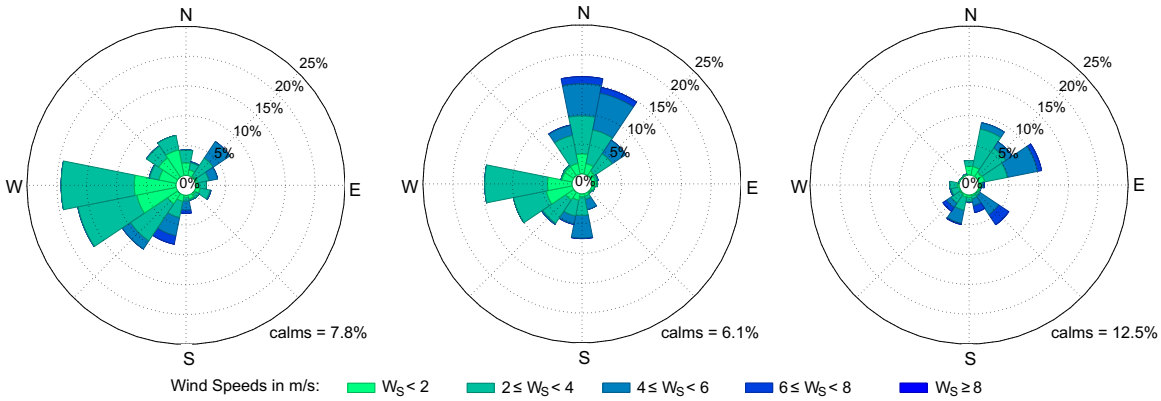

Fig. 2. Wind roses for the period of the field measurements in (left to right) April, July and January respectively. Calms were defined as wind speeds ≤1 m s^{-1}.

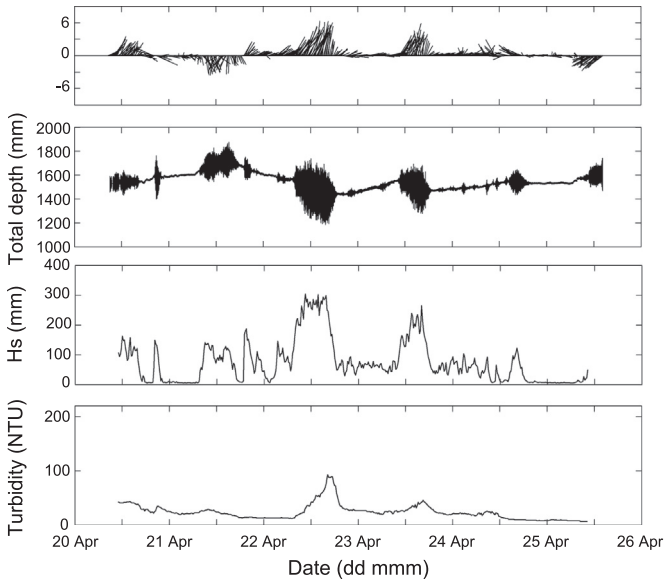

Fig. 3. Time series of wind vectors (top panel, origins on axis), total water depth (second panel), significant wave heights (third panel) and turbidity (bottom panel) at wave pole AP3 (refer Fig. 1(b)) during April 2013.

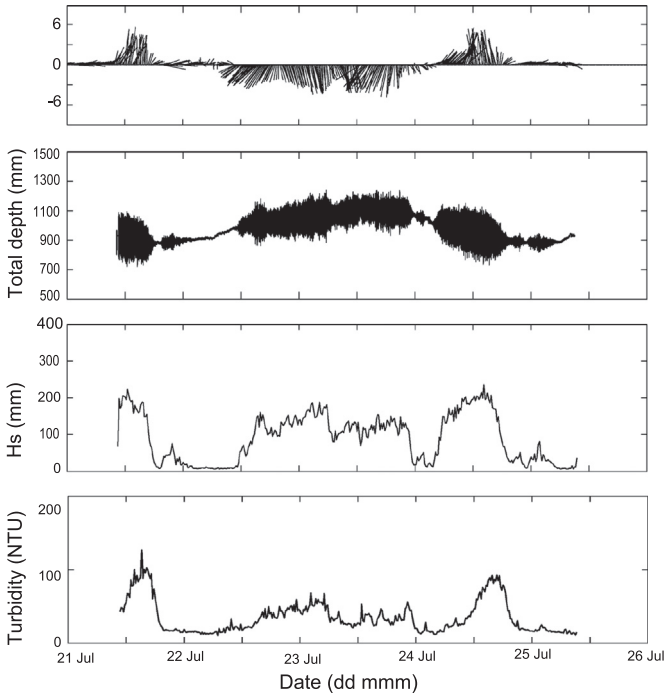

Fig. 4. Time series of wind vectors (top panel, origins on axis), total water depth (second panel), significant wave height (third panel) and turbidity (bottom panel) at wave pole JP0 (refer Fig. 1(b)) during July 2013. The water level, significant wave height and turbidity time series for JP3 closely resemble JP0 and have not been included.

3. Results

3.1. Wind and waves

During the field experiments wind directions regularly alternated between north/north-easterly to south/south-westerly (Fig. 2). We observed a diurnal wind pattern of low night-time speeds (typically $<4\ m\ s^{-1}$) to high mid-day speeds (typically $>6\ m\ s^{-1}$) (Figs. 3–5). Night time winds were thermally driven land breezes predominantly originating from the west. This pattern is

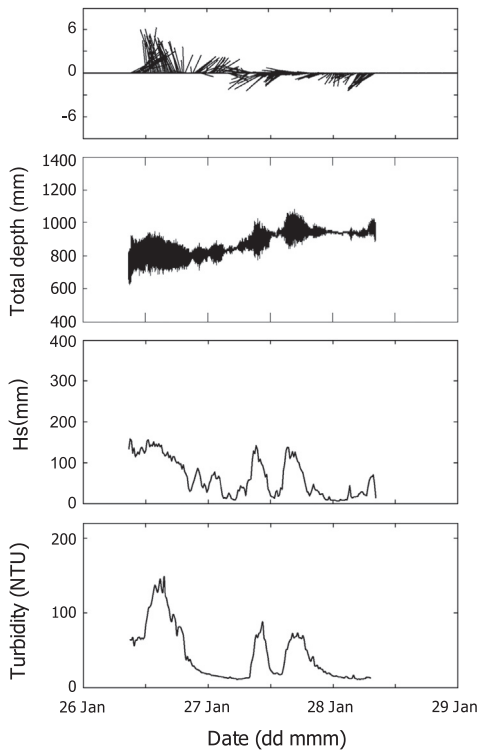

Fig. 5. Time series of wind vectors (top panel, origins on axis), total water depth (second panel), significant wave height (third panel) at wave pole JAN3 (refer Fig. 1 (b)) during January 2014. The turbidity time series (bottom panel) was measured simultaneously at wave pole JAN2.

Table 1
Range of still water depth, total depth, wind fetch, and significant wave height at sampling locations (refer Fig. 1(b)). Still water depths exclude waves while total depths include waves. No wave measurements were made at site JAN2 and still water depths were estimated using a survey staff.

Sampling locations	SW depth (mm)	Total depth (mm)	Fetch (mm)	H_s (mm)
AP3	1410–1730	1180–1880	50–11000	10–350
JP0	820–1070	660–1190	700–10200	10–240
JP3	1850–2090	1720–2500	1400–9700	10–380
JAN2	1350–1600	–	600–9600	–
JAN3	740–970	620–1010	700–10200	10–300

characteristic of Lake St Lucia. Maximum fetches during our experiments were about 10 km and mostly associated with winds from northerly directions (Table 1).

In April strong winds persisting for approximately 12 h periods were repeatedly observed during the day. The third day of the study coincided with passage of a south-westerly storm while the last two days were relatively calmer (refer to Fig. 3). In July a period of persistent wind lasting approximately 36 h and varying in direction from north-easterly to north-westerly was observed on the second day. Wind directions were overall strongly aligned towards the northern and southern directions (Fig. 4). In January measured wind speeds were high from mid-day of the first day into the night, only dying down during the middle of the second day. The characteristic daily alternation in direction was not apparent (Fig. 5).

Significant wave heights or wave energy measured over the course of the study increased almost immediately in response to changes in wind speed and direction. As expected high wind speeds acting in directions aligned with larger fetches resulted in

more pronounced wave events and greater observed significant wave heights (Figs. 3–5). The variation observed during peak H_s events may be attributed to the effect of gusts and slight variations in wind speed and direction as outlined in our previous study (Zikhali et al., 2014). Water depths for each pole site changed in response to changes in wind direction with site JP3 having the greatest average depth (Table 1). The wave fields had a narrow frequency range, with the dominant wave-period about 2 s.

3.2. Turbidity and SSC

Turbidities in South Lake responded quickly to wave events and thus showed a high variability, in particular displaying a diurnal pattern corresponding to that of the wind and waves (Figs. 3–5). A cross-correlation analysis indicated a delay of about 1 h between changes in wave action and corresponding changes in turbidity (and hence the SSC).

We observed that turbidity dynamics at pole AP3 were less sensitive to wave height changes compared to other locations (Figs. 3–5). The peak H_s observed at site AP3 was just under 200 mm while turbidities mostly remained below 50 NTU. Turbidity levels only rose above 100 NTU during a southerly storm on the third day. This is linked to a peak H_s of 300 mm at the time. A similar southerly high wind on the fourth day resulted in a lesser increase in turbidity, with H_s peaking at 250 mm.

In July strong southerly winds resulted in frequent spikes in turbidity. Peak H_s reached 200 mm at site JP0 corresponding to a turbidity of about 100 NTU. Similar northerly high winds caused peak H_s to reach 150 mm and resulted in gradual increases in turbidity. The turbidity and corresponding SSC time series in July (JP0 and JP3) displayed the same overall pattern with the shallower site JP0 showing slightly higher peak turbidities than site JP3 (Fig. 6).

The turbidity time series measured in January at site JAN2 was consistent with the wave time series from site JAN3 (Fig. 5). Peaks in turbidity again coincided with the highest significant waves where a peak H_s of approximately 150 mm was associated with turbidities of about 150 NTU.

Measured vertical turbidity profiles in April 2013 showed mainly uniform values over most of the water column, but with some significant variations observed in isolated cases (Fig. 7). These exceptions were at deeper locations and at times when wind or wave conditions were rapidly changing thus resulting in transient, incomplete vertical mixing. Overall, the data generally supports an assumption of a vertically well mixed water column in relatively stable conditions. We note that steep turbidity gradients were evident near the lake bed for profiles measured in muddy regions. These are associated with a layer of soft fluid mud that was particularly evident at the deeper muddy central regions of South Lake (near site JP3 – refer to Fig. 1). The depth of the fluid mud layer at T1 and T2 was estimated to be in the range 0.5–0.8 m.

3.3. Sediment size characteristics

Particle size characteristics for bed sediments collected from various sites are summarised in Table 2. They show a range from predominantly sandy sediments (D_{50} = 290 μm) at site AP3, to fine mud (D_{50} = 11 μm) at JAN3, with more mixed characteristics at sites JP0, JP3, and JAN3 (76 μm ≤ D_{50} ≤ 260 μm). The spatial distribution of sediment types reported by Fortuin (1992) (see also Perissinotto et al., 2013, Fig. 9.5) and shown in Fig. 1 is broadly consistent with our results.

Particle size characteristics for suspended sediments collected at various locations are summarised in Table 3. In contrast to the spatial variability in the bed sediment samples, the suspended sediment samples had more uniform characteristics and were strongly dominated by particles with a mud classification (D_{50} ≤ 63 μm). The uniformity of the suspended sediment size characteristics in part justifies the use of a constant settling velocity to model their behaviour.

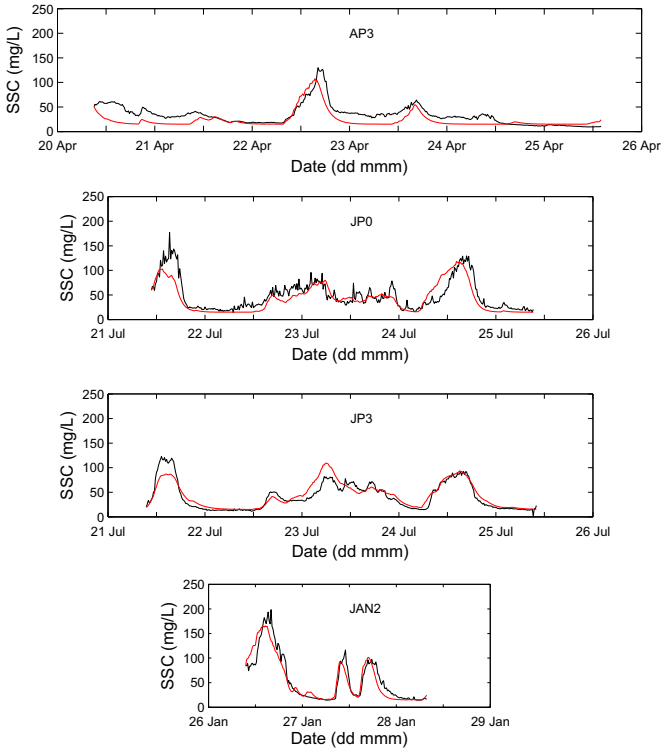

Fig. 6. Observed SSC (−) and modelled SSC (red/dashed line) for each sampling station set up in South Lake during the course of the study. Stations AP3 and JP0 were located in a predominantly sandy region, while stations JP3 and JAN2 had a muddier bed composition (refer Fig. 1 and Table 2).

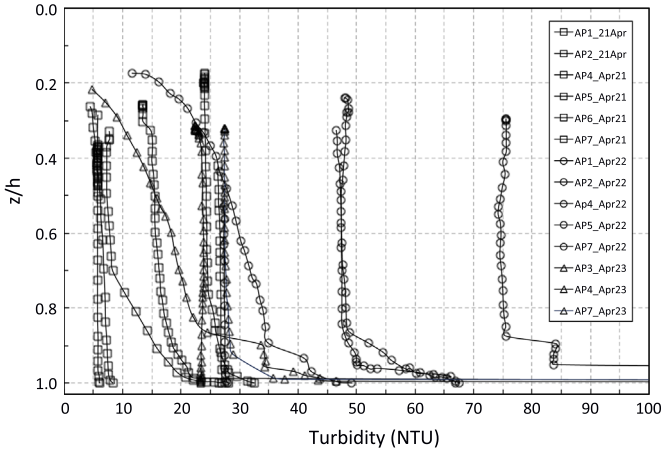

Fig. 7. Measured vertical turbidity profiles at multiple positions (sites AP1–AP7) within St Lucia's South Lake in April 2013. Profiles measured on the 21st are indicated by □, the 22nd by ◯, and on the 23rd by △. Refer Fig. 3 for wind and wave data for the same dates.

3.4. SSC model results

The Luettich et al. (1990) model was used to simulate sediment resuspension using observed H_s and h together with assumed model parameters H_c, w_s, c_o and K. Observed turbidity was related to SSC using a derived calibration curve (see Section 2.2) and inferred SSC data was compared to modelled SSC.

Table 2
Particle size distributions of bed core samples, sediment classification and model K value at the different pole sites. The $D_{10/50/90}$ values are the 10th, 50th and 90th percentiles of particle diameters in each sample, respectively.

Pole site	D_{10} (μm)	D_{50} (μm)	D_{90} (μm)	Mud %	Sand %	Class	K mg l^{-1}
AP3	97	290	560	8	92	Sand	5000
JP0	10	220	420	24	76	Muddy sand	2700
JP3	3.4	76	310	50	50	Muddy sand	4800
JAN3	8.9	260	590	30	70	Muddy sand	–
JAN2	2.7	11	68	90	10	Mud	9000

Table 3
Suspended sediment size distributions for water samples from April 2013 (AP2, AP3, AP5, AP6, T1, T2) and January 2014 (JAN2). For pole positions see Fig. 1(b).

Sampling Location	Particle size (μm)			Classification	
	D_{10}	D_{50}	D_{90}	Mud %	Sand %
AP2	3.5	11	42	95	5
AP3	3.7	11	39	96	4
AP5	3.2	10	47	94	6
AP6	4.2	13	44	94	6
T1	2.8	8.3	26	96	4
T2	2.4	7.0	15	98	2
JAN2	2.9	8.9	52	92	8

The model reproduced the general trends in "observed" SSC i.e. the timing of increases and decreases in SSC were correctly reproduced in all cases. At low wind speeds the model correctly ignored short-lived increases in wave height and the SSC maintained lower values, mirroring the observations (Fig. 6).

The estimated model parameters are given in Table 4. Only the parameter K was allowed to vary between sites, and values ranged from 2700 mg l^{-1} at JP0 to 9000 mg l^{-1} at JAN3. The K values increased with decreasing bed sediment size with the exception of site AP3 (Table 2).

When SSC fell below approximately 50 mg l^{-1} we observed a decrease in the settling velocity as indicated by a slowed decrease in SSC (Fig. 6). A model using a constant w_s cannot accurately mimic this behaviour. Model simulations were done to test the effects of using a variable settling velocity linked to the SSC in the form $w_s(c) = w_s(c/c_0 - 1)^{\alpha}$ where w_s is a constant reference settling velocity and exponent α controls the sensitivity to SSC variations. This implies that when concentrations drop to background levels, w_s reduces to zero. The variable settling velocity only marginally improved the overall model performance and is thus omitted from the results presented here.

Model performance improved as site mud content increased (refer to Table 2 for site classification and Table 5 for error estimates). The root mean square error for the different sites ranged between 12 and 19 mg l^{-1} and was below 10% of maximal SSC observed (Table 5). The model gave its highest agreement and efficiency indices for sites JAN2 and JP3 (both indices>0.8), which had the highest depths and mud contents (Table 5). The model performed poorest at site AP3 (agreement and efficiency indices <0.6), which consisted of a coarser bed sediment, lower mud content and an average depth similar to JAN2. It should be noted that the original (Luettich et al., 1990) model was calibrated in Lake Balaton which has a high silt content bed composition.

Table 4
Parameters of the resuspension model derived for this study. Parameter K was allowed to vary from site to site to reflect different resuspension characteristics.

Model parameters	Values
c_o (mg l^{-1})	15
H_c (cm)	3
K (mg l^{-1})	2700–9000
n (dimensionless)	2
w_s (cm s^{-1})	0.02

Table 5
Error analysis of modelled SSC against observed SSC.

Polestation	Error parameter	Value
AP3	Agreement index	0.59
	Efficiency index	0.38
	RMSE (mg l^{-1})	16
	observed mean (mg l^{-1})	33
	modelled mean (mg l^{-1})	24
JP0	Agreement index	0.73
	Efficiency index	0.64
	RMSE (mg l^{-1})	19
	Observed mean (mg l^{-1})	49
	Modelled mean (mg l^{-1})	42
JP3	Agreement index	0.81
	Efficiency index	0.82
	RMSE (mg l^{-1})	12
	Observed mean (mg l^{-1})	42
	Modelled mean (mg l^{-1})	44
JAN2/3	Agreement index	0.85
	Efficiency index	0.88
	RMSE (mg l^{-1})	16
	Observed mean (mg l^{-1})	57
	Modelled mean (mg l^{-1})	55

4. Discussion

This study is the first to measure and model SSC dynamics and wave characteristics in Lake St Lucia. The measured turbidity time series showed variability from sub-hourly to daily time scales which is not resolved by monitoring studies that typically measure turbidity on monthly or seasonal time scales. The study confirms that when wind speeds increase during the day surface waves rapidly develop leading to corresponding increases in water column turbidity and SSC after a short delay. Conversely, in the evenings when the wind dies down most of the suspended particulate matter settles from the water column with a corresponding decrease in turbidity and SSC. This results in a highly variable environment for the lake's organisms. These inhabitants are required to adjust to frequent changes in light availability for processes like production (microalgae) or visibility-based hunting (fish). The varying SSC may also influence the feeding behaviour of organisms such as zooplankton or macro-zoobenthos (Cloern,

1987; Cyrus and Blaber, 1987; Carrasco et al., 2013).

To model SSC dynamics in Lake St Lucia, we used wind-driven wave activity as the primary resuspension mechanism at various sites with differing bed composition. Sediment resuspension events in shallow lakes without significant advective currents are limited by wave induced shear stress and/or bed composition (Jin and Ji, 2001; Qian et al., 2011; Zheng et al., 2015). Ross and Mehta (1989) and Wu et al. (2013) suggest that the energy required for turbulent mixing and uniform concentration over most of the water column is provided mainly by wind-driven wave activity. Schoen et al. (2014) modelled the wind-driven advection currents in St Lucia's South Lake and found them to be typically <0.2 m s^{-1}. This supports the assumption that most suspended sediment is introduced into the water column due to local wave activity rather than advective current effects (Cozar et al., 2005; Wu et al., 2013). Nevertheless the observed uniformity of the suspended sediment size characteristics suggests that wind-driven circulation may play an important role in distributing these sediments horizontally across the lake basin. After these fine muddy sediments settle in sandy areas during night-time calms, they would be quickly re-suspended by waves when windy conditions resume during daytime. This conjecture suggests that the supply of resuspendable material in sandy regions could be limited by this mechanism.

Model optimisation resulted in a unique resuspension parameter K for each location in our study. A higher K value corresponds to higher equilibrium SSC, i.e. higher bed erodibility for a given wave energy (see Eq. (2)). Bed shear resistance is known to increase with layer depth, bed cohesiveness and structural integrity (Ross and Mehta, 1989). The highest K value was observed at the muddiest site (9000 mg l^{-1} at JAN2) concurring with the general theory of muddy substrates having higher erodibility than sand. However, the sandiest site (AP3) showed the second highest K (5000 mg l^{-1}), whereas the lowest value of 2700 mg l^{-1} was found at JP0 where the bed consisted of 24% mud and 76% sand (see Table 2). This lower erosion rate at JP0 may be attributed to a shift in the bed structure from non-cohesive to cohesive with increasing mud content due to the infilling of inter-granular space by fine clay/silt (van Ledden et al., 2004). Increases in bed mud content beyond 30–50% should consequently lower shear resistance due to corresponding decrease in sediment bulk density (Grabowski et al., 2011). Differences in layer depth may also cause differences in model K. For an undisturbed bed initial resuspension rates may be high but then decrease as underlying layers with higher critical shear strength are exposed, thus reducing erosion rates (Aberle et al., 2004). This is analogous to having a limited supply of resuspendable material which would also result in a lower K value.

In St Lucia's South Lake, we observed a thick fluid mud layer ($\sim$ 0.5 m) in areas classified as muddy, but not in those classified as sandy. This mud layer was weakly bonded to the bed similar to a mud layer observed by Wu et al. (2013) in the eutrophic Taihu Lake. Bed shear resistance was expected to be low in these regions while peak equilibrium SSC was expected to be high. The muddier regions (poles JP3 and JAN2) were expected to display higher turbidities than the sandier regions (poles JP0 and AP3). This was true for the muddy JAN2 location where turbidities reached the highest values (150 NTU) of all stations. For the sandy AP3 location turbidities only reached 100 NTU during a 300 mm H_s event. Peak turbidities observed at JP3 were unexpectedly slightly lower than those observed at JP0. Ross and Mehta (1989) suggest the presence of a stable lutocline may reduce mixing rates within the water column above. Thus, the persistent mud layer present around JP3 but not JP0 may have counteracted higher erodibility at this site. The water at JP3 was also twice as deep as at JP0 which could also have played a role in this result.

Using a single parameter (K) to describe the resuspension dynamics does not allow the model to distinguish between physical and biological effects on resuspension. Thus, differences in estimated K between sites could also be due to changes in benthic communities. During the study period microphytobenthos biomass was below 20 mg m^{-2} at most sites (data not shown) and thus below a value that would suggest significant effects on erodibility (Le Hir et al., 2007). The zoobenthos community in Lake St Lucia is diverse and at times high animal densities are observed (Mackay et al., 2010; Perissinotto et al., 2013), however we do not have specific information for our study period and sites. The large population of *Hippotamus* in Lake St Lucia may also increase turbidity in areas with high activity (Perissinotto et al., 2013).

The Luettich model used in our study is a depth-averaged box model and thus assumes a vertically well mixed water column. Measurements shown in Fig. 7 mainly show no turbidity gradient with depth down to the near-bed lutocline layer where a sudden increase in turbidity occurred. This suggests that the water column is usually well mixed in Lake St Lucia. This is consistent with the observations made in Changjiang Estuary by Shi et al. (1996) where low vertical SSC gradients were observed during flood tides. Vertical gradients seem most likely to develop during transient periods with rapidly increasing or decreasing wave energy where there is a time delay before full vertical mixing or settling of resuspended sediment over the water column.

Ross and Mehta (1989) suggested a uniform settling velocity w_s for SSC below 400 mg l^{-1}. Maine (2011) conducted a study on the settling velocity of sediment collected from South Lake. Our results agree with a settling velocity <0.05 cm s^{-1} that he identified for an SSC of 100 mg l^{-1}. Analysis of the measured turbidity data in our study revealed an accelerated decrease in turbidity from the peak values after high wave events, with slower decay rates at low turbidities in calmer conditions. Attempts to introduce a variable settling velocity linked to SSC were able to mimic this behaviour, but overall model performance did not improve significantly. Sediment deposition of cohesive sediments is known to depend on factors other than SSC including organic content, turbulence and flocculation (e.g. Soulsby et al., 2013; Liu et al., 2014). Incorporating these and other factors to model a variable settling velocity is physically justifiable and may improve the accuracy of the model somewhat but with added complexity.

Our modelling method followed the box model formulation of Luettich et al. (1990) which balances resuspension by wave-driven shear stresses and gravity-driven settling to describe SSC dynamics. This simplified process-based model allowed us to incorporate the influence of bed composition and depth variations on resuspension dynamics. The model requires wave data, either measured or modelled. Other approaches have used purely empirical methods (Measures and Tait, 2008), and more complex process-based models have included the effects of bed roughness and multiple layers (Nino et al., 2003; Widdows et al., 2006). Henry and Minier (2014) used a stochastic model to predict when hydrodynamic forces exceed bed-particle adhesive forces. While these alternative models have been shown to be effective the results of this study suggest that a simple box model, with limited parameter tuning, is also capable of producing accurate simulations of SSC variations in a complex shallow system.

5. Conclusion

This study used field experiments to elucidate the short timescale wave-driven suspended sediment dynamics for a large shallow lake with complex morphology and variable bed sediments. It is the first such study undertaken in the Lake St Lucia system and provides insights that should be applicable to similar systems worldwide. Features of this system include wet and dry cycle variations in water levels, strong wind-driven inter-basin

water exchanges, and wave-driven resuspension of fine sediments with associated high turbidities. The measurements highlight strong spatiotemporal variability in suspended sediment concentrations. A simple model with a single spatially varying parameter has been shown to be capable of adequately describing the SSC variations. The results are important for understanding and predicting the ecological dynamics at Lake St Lucia and other similar large shallow systems. The study has also revealed issues that require further investigation. For example additional field experiments and/or modelling work could help clarify the various factors that influence the resuspension process (as described by the parameter K in the simple model used here) as well as the relative importance of local resuspension versus advective redistribution in spatiotemporal SSC dynamics.

Acknowledgements

Thanks to iSimangaliso Wetland Park Authority for supporting the research; National Research Foundation (Grant no. 91347) and SANPAD (Grant no 10/90) for funding; South African Weather Service for wind data; Caroline Fox for field support, Zane Thackeray for data loggers; Henk-Jan Verhagen for his MATLAB script; Julia Schoen for help with field work and data analysis; Sydney Mpungose and Logan Govender for fabricating field equipment and Fathima Ali for laboratory assistance. K.T. was supported by an NRF postdoctoral fellowship (Grant no. 85165). Thanks also to an anonymous reviewer whose detailed commentary significantly improved our paper.

References

Aberle, J., Nikora, V., Walters, R., 2004. Effects of bed material properties on cohesive sediment erosion. Mar. Geol. 207, 83–93.
Bailey, M.C., Hamilton, D.P., 1997. Wind induced sediment resuspension: a lake-wide model. Ecol. Modell. 99, 217–228.
Benfield, M.C., Bosschieter, J., Forbes, A.T., 1990. Growth and emigration of Penaeus indicus H. Milne-Edwards (Crustacea: Decapoda: Penaeidae) in the St. Lucia estuary, Southern Africa. Fish. Bull. 88, 21–28.
Brand, A., Lacy, J.R., Hsu, K., Hoover, D., Gladding, S., Stacey, M.T., 2010. Wind-enhanced resuspension in the shallow waters of South San Francisco Bay: mechanisms and potential implications for cohesive sediment transport. J. Geophys. Res. 115, 1–15.
Carrasco, N., Perissinotto, R., Jones, S., 2013. Turbidity effects on feeding and mortality of the copepod Acartiella natalensis (Connell and Grindley, 1974) in the St. Lucia Estuary, South Africa. J. Exp. Mar. Biol. Ecol. 446, 45–51.
Castaing, P., Allen, G.P., 1981. Mechanism controlling seaward escape of suspended sediment from the Gironde: a macrotidal estuary in France. Mar. Geol. 40, 101–118.
Cloern, J., 1987. Turbidity as a control on phytoplankton biomass and productivity in estuaries. Cont. Shelf Res. 7, 1367–1381.
Cozar, A., Galvez, J.A., Hull, V., Garcia, C.M., Loiselle, S.A., 2005. Sediment resuspension by wind in a shallow lake of Esteros del Ibera (Argentina): a model based on turbidimetry. Ecol. Modell. 186, 63–76.
Cyrus, D.P., 1988. Turbidity and other physical factors in natal estuarine systems. Part 2. Estuarine lakes. J. Limnol. Soc. S. Afr. 14, 72–81.
Cyrus, D.P., Blaber, S.J.M., 1987. The influence of turbidity on juvenile marine fish in estuaries. Part 2. Laboratory studies, comparisons with field data and conclusions. J. Exp. Mar. Biol. Ecol. 109, 71–91.
Dyer, K.R., 1986. Coastal and Estuarine Sediment Dynamics. Wiley & Sons, Chichester, UK.
Folk, R.L., 1954. The distinction between grain size and mineral composition in sedimentary-rock nomenclature. J. Geol. 62 (4), 344–359.
Fortuin, H.H.G., 1992. Sediment distribution patterns in Lake St Lucia. CSIR Division of Earth, Marine and Atmospheric Science & Technology, Research Report 712.
Grabowski, R.C., Droppo, I.G., Wharton, G., 2011. Erodibility of cohesive sediment: the importance of sediment properties. Earth-Sci. Rev. 105, 101–120.
Green, M.O., 2011. Very small waves and associated sediment resuspension on an estuarine intertidal flat. Estuar., Coast. Shelf Sci. 93, 449–459.
Healy, T.R., Wang, Y., Healy, J.-A. (Eds.), 2002. Muddy Coasts of the World: Processes, Deposits and Function. Elsevier, Amsterdam, Netherlands.
Henry, C., Minier, J.P., 2014. Progress in particle resuspension from rough surfaces by turbulent flows. Prog. Energy Combust. Sci. 45, 1–53.
Hutchison, I.P.G., Pitman, W.V., 1977. Lake St Lucia: mathematical modelling and evaluation of ameliorative measures. Civil Eng. S. Afr. 19, 75–82.
Jin, K.R., Ji, Z.G., 2001. Calibration and verification of a spectral wind-wave model for Lake Okeechobee. Ocean Eng. 28, 571–584.
Lawrie, R.A., Stretch, D.D., 2011a. Anthropogenic impacts on the water and salinity budgets of St Lucia estuarine lake in South Africa. Estuar., Coast. Shelf Sci. 93, 58–67.
Lawrie, R.A., Stretch, D.D., 2011b. Occurrence and persistence of water level/salinity states and the ecological impacts for St Lucia estuarine lake, South Africa. Estuar., Coast. Shelf Sci. 95, 67–76.
Legates, D.R., McCabe Jr., G.J., 1999. Evaluating the use of "goodness-of-fit" measures in hydrological and hydroclimactic model validation. Water Resour. Res. 35, 233–241.
Le Hir, P., Monbet, Y., Orvain, F., 2007. Sediment erodability in sediment transport modelling: Can we account for biota effects?. Cont. Shelf Res. 27, 1116–1142.
Liu, J.H., Yang, S.L., Zhu, Q., Zhang, J., 2014. Control on suspended sediment concentration profiles in the shallow and turbid Yangtze Estuary. Cont. Shelf Res. 90, 96–108.
Luettich, R.A., Harleman, D.R.F., Somlydody, L., 1990. Dynamic behaviour of suspended sediment concentration in a shallow lake perturbed by episodic wind events. Limnol. Oceanogr. 35, 1050–1067.
Lundkvist, M., Grue, M., Friend, P.L., Flindt, M.R., 2007. The relative contributions of physical and microbiological factors to cohesive sediment stability. Cont. Shelf Res. 27, 1143–1152.
Mackay, F., Cyrus, D., Russell, K.-L., 2010. Macrobenthic invertebrate responses to prolonged drought in South Africa's largest estuarine lake complex. Estuar., Coast. Shelf Sci. 86, 553–567.
Maine, C., 2011. The Flocculation Dynamics of Cohesive Sediments in the St Lucia and Mfolozi Estuaries, South Africa. University of KwaZulu-Natal, South Africa.
Measures, R., Tait, S., 2008. Quantifying the role of bed surface topography in controlling sediment stability in water-worked grave deposits. Water Resour. Res. 44.
Mikes, D., Verney, R., Lafite, R., Belorgey, M., 2002. Controlling factors in estuarine flocculation processes. Experimental results with material from the Seine Estuary. J. Coast. Res. 41, 82–89.
Nino, Y., Lopez, F., Garcia, M., 2003. Threshold for particle entrainment into suspension. Sedimentology 50, 247–263.
Partheniades, E., 1965. Erosion and deposition of cohesive soils. ASCE J. Hydraul. Div. 91, 105–138.
Partheniades, E., 2009. Cohesive Sediments in Open Channels. Elsevier, Oxford, UK.
Perissinotto, R., Stretch, D.D., Taylor, R.H. (Eds.), 2013. Ecology and Conservation of Estuarine Ecosystems: Lake St. Lucia as a Global Model. Cambridge University Press, Cambridge, UK.
Ravens, T., 1997. Sediment Resuspension in Boston Harbor. Massachusetts Institute of Technology, Boston, United States of America.
Qian, J., Zheng, S., Wang, P., Wang, C., 2011. Experimental study on sediment resuspension in Taihu lake under different hydrodynamic disturbances. J. Hydrodyn. 23 (6), 825–833.
Ross, M.A., Mehta, A.J., 1989. On the mechanics of Lutoclines and fluid mud. J. Coast. Res. SE 5, 51–62.
Scheffer, M., 1998. Ecology of Shallow Lakes. Chapman & Hall, London.
Schoen, J., Stretch, D.D., Tirok, K., 2014. Wind-driven circulation in a shallow estuarine lake: St Lucia, South Africa. Estuar., Coast. Shelf Sci. 146, 49–59.
Shi, Z., Ren, L.F., Lin, H.L., 1996. Vertical suspension profile in the Changjiang Estuary. Mar. Geol. 130, 29–37.
Soulsby, R.L., Manning, A.J., Spearman, J., Whitehouse, R.J.S., 2013. Settling velocity and mass settling flux of flocculated estuarine sediments. Mar. Geol. 339, 1–12.
van Ledden, M., van Kesteren, W.G.M., Winterwerp, J.C., 2004. A conceptual framework for the erosion behaviour of sand-mud mixtures. Cont. Shelf Res. 24, 1–11.
Whitfield, A., Taylor, R., Fox, C., Cyrus, D., 2006. Fishes and salinities in the St Lucia estuarine system—a review. Rev. Fish Biol. Fish. 16, 1–20.
Widdows, J., Brinsley, M.D., Pope, N.D., Staff, F.J., Bolam, S.G., Somerfield, P.J., 2006. Changes in biota and sediment erodability following the placement of fine dredged material on upper intertidal shores of estuaries. Mar. Ecol. Prog. Ser. 319, 27–41.
Willmott, C.J., 1981. On the validation of models. Phys. Geogr. 2, 184–194.
Wolanski, E., 2007. Estuarine Ecohydrology. Elsevier, Amsterdam, Netherlands.
Wu, D., Hua, Z., 2014. The effect of vegetation on sediment resuspension and phosphorus release under hydrodynamic disturbance in shallow lakes. Ecol. Eng. 69, 55–62.
Wu, T., Qin, B., Zhu, G., Zhu, M., Li, W., Luan, C., 2013. Modelling of turbidity dynamics caused by wind-induced waves and current in the Taihu Lake. Int. J. Sediment Res. 28, 139–148.
Zheng, S., Wang, P., Wang, C., Hou, J., 2015. Sediment resuspension under action of wind in Taihu Lake, China. Int. J. Sediment Res. 30, 48–62.
Zikhali, V., Tirok, K., Stretch, D.D., 2014. Wind driven waves in a shallow estuarine lake with muddy substrates: St Lucia, South Africa. J. Coast. Res. SI 70, 729–735.